JACS
JOURNAL OF THE AMERICAN CHEMICAL SOCIETY

ARTICLE

pubs.acs.org/JACS

The Particle Size Effect on the Oxygen Reduction Reaction Activity of Pt Catalysts: Influence of Electrolyte and Relation to Single Crystal Models

Markus Nesselberger,[†] Sean Ashton,[†] Josef C. Meier,[‡] Ioannis Katsounaros,[‡] Karl J. J. Mayrhofer,[‡] and Matthias Arenz*[,†]

[†]Department of Chemistry, University of Copenhagen, Universitetsparken 5, DK-2100 Ø Copenhagen, Denmark

[‡]Max-Planck-Institut für Eisenforschung GmbH, Max-Planck-Strasse 1, D-40237 Düsseldorf, Germany

Supporting Information

ABSTRACT: The influence of particle size on the oxygen reduction reaction (ORR) activity of Pt was examined in three different electrolytes: two acidic solutions, with varying anionic adsorption strength ($HClO_4$ < H_2SO_4); and an alkaline solution (KOH). The experiments show that the absolute ORR rate is dependent on the supporting electrolyte; however, the relationship between activity and particle size is rather independent of the supporting electrolyte. The specific activity (SA) toward the ORR rapidly decreases in the order of polycrystalline Pt > unsupported Pt black particles (~30 nm) > high surface area (HSA) carbon supported Pt nanoparticle catalysts (of various size between 1 and 5 nm). In contrast to previous work, it is highlighted that the difference in SA between the individual HSA carbon supported catalysts (1 to 5 nm) is rather trivial and that the main challenge is to understand the significant differences in SA between the polycrystalline Pt, unsupported Pt particles, and HSA carbon supported Pt catalysts. Finally, a comparison between measured and modeled activities (based on the distribution of surface planes and their SAs) for different particle sizes indicates that such simple models do not capture all aspects of the behavior of HSA carbon supported catalysts.

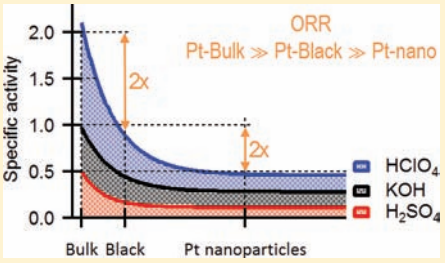

INTRODUCTION

For many decades the structure−activity relationship of surfaces has been one of the main research topics in catalysis, and the ability to prepare and utilize well-defined single crystal surfaces has led to a significant advancement in our understanding of catalytic processes.[1−3] In gas-phase catalysis studies, focus is typically placed on the influence of the catalyst surface structure on the adsorption and desorption of reactants, intermediates, and reaction products. In electrocatalysis, however, an additional factor must be considered, namely, the influence of surface structure on the adsorption of species that are not directly involved in the reaction but nevertheless influence the reaction rate, so-called spectator species.[3−5] This phenomenon has, for example, been nicely revealed by comparing the oxygen reduction reaction (ORR) rates of the three different low-indices Pt single crystal surfaces in aqueous electrolytes of different adsorption strengths. In a weakly adsorbing electrolyte such as perchloric acid, Pt(111) is considerably more active than Pt(100);[6] however Pt(111) is the least active surface in sulfuric acid solution.[4] This finding is rationalized by the strong adsorption of sulfate anions—as spectators—on the hexagonal (111) surface.

In contrast to single crystal model electrodes, industrial catalysts are usually composed of finely dispersed catalyst particles anchored onto a support (in order to maximize the accessible surface area per mass of the catalyst) and do not, in general, possess extended crystal facets. Nonetheless, the influence of the particle size of such particulate catalysts on the reaction rate of structure-sensitive reactions has been traditionally related to the structure−activity relationship of single crystals.[7,8] Early experimental data of Ross et al.[9] and Boudart et al.[10] on the influence of the size of carbon supported Pt nanoparticles (NPs) on the ORR activity were summarized and discussed by Kinoshita.[11] The data indicated that the specific activity (SA), i.e. the reaction rate normalized to the platinum surface area of Pt NPs, decreases in sulphuric and phosphoric acid electrolyte with decreasing particle size from 12 to 2.5 nm, a trend which was found to be more pronounced toward small particles. The mass activity (MA) defined as the reaction rate per gram of Pt exhibits a maximum at a particle size of around 3 nm in these studies. These experimental findings were explained by Kinoshita[11] on the basis of a model that assumed Pt NPs possess a truncated cuboctahedral structure, whose distribution of surface planes changes with particle size, particularly for particle sizes below 5 nm.[12,13] Because of the strong adsorption of anions on the (111) face, the (100) face was proposed to play the more dominant role in the electrocatalytic reaction,[11] a conclusion that was supported by the correlation between the peak MA and the

Received: July 27, 2011
Published: September 27, 2011

mass averaged distribution of the (100) crystal face. In more recent studies it has been reported by several groups, including the authors, that high catalyst dispersion and small particle size also detrimentally influence the SA for the ORR in weakly adsorbing electrolytes. However, the particle size effect exhibited a different trend than in the previous studies, whereby the effect was more pronounced toward larger particles sizes, whereas toward decreasing particle sizes the differences in SA were smaller.[14−18] These newer studies benefitted from employing the recently developed thin-film RDE technique[19] avoiding oxygen concentration profiles within the catalyst layer. The results seem rather intriguing if we consider the different activities of single crystal facets in various electrolytes, and a refined explanation of the particle size effect was proposed based on a shift of the potential of zero total charge (pztc) with the particle size and a concomitant alteration of the adsorption potential of spectator species.[16] It is noteworthy, however, that despite the qualitative analogy between pztc and activity, in further studies no quantitative agreement could be reached.

In the work presented here, we examine the influence of the size of Pt NPs on the ORR in different electrolyte solutions with varying anionic adsorption strength. In comparison to our previous study,[16] we utilize an improved experimental setup and methodology,[20,21] using analog compensation of the electrolyte resistance and a background subtraction that eliminates the significant capacitive current contributions arising from the high surface area (HSA) carbon support. Based on these new experimental results, we discuss one of the still prevailing explanations of the particle size effect that relies on the extrapolation of single crystal data to particle facets and identify its respective weaknesses.

EXPERIMENTAL SECTION

Catalyst Material. Four different HSA carbon supported catalysts provided by TKK (Tokyo, Japan), a Pt-black catalyst provided by Umicore AG, and a polycrystalline platinum sample (5 mm diameter) were investigated. The carbon support of the catalysts is identical for all samples. According to TKK analysis, the HSA carbon supported catalysts have four different average particle sizes, i.e. about 1 nm (HS_1), 2 nm (HS_2), 2−3 nm (HS_3), and 4−5 nm (HS_5) which are consistent with their electrochemical surface area (ECSA) values and our analysis by TEM and XRD. The samples HS_1, HS_2, and HS_5 are the same as those used in our previous studies.[16,17,22] The mean particle size for the Pt-black catalyst was given as 30 nm which corresponds to the crystallite size established by XRD. TEM analysis however shows that Pt agglomerates with a broad size distribution are formed. In order to use a classification which is more unambiguous than the mean particle size, the catalysts are additionally characterized by their ECSA.

Electrochemical Measurements. The catalyst powders were ultrasonically dispersed in ultrapure water to a concentration of 0.14 mg_{Pt} cm^{-3} for at least 10 min. Before each measurement the catalyst suspension was again put into the ultrasonic bath for 3 min. For the ORR measurements, a volume of 20 μL of the suspension was pipetted onto a polished glassy carbon substrate (5 mm diameter, 0.196 cm^2 geometrical surface area) leading to a Pt loading of 14 μg_{Pt} cm^{-2} for the catalyst sample. The catalyst suspension was then dried onto the glassy carbon electrode in a nitrogen gas stream. The electrochemical measurements were conducted in a three-compartment electrochemical Teflon cell, using a rotating disk electrode setup and a home-built potentiostat with analog compensation of the solution resistance.[20] A saturated Calomel electrode and a graphite rod were used as reference and counter electrodes, respectively. All potentials in the paper are expressed with respect to the reversible hydrogen electrode (RHE) potential, which was experimentally determined for each measurement series. The electrolyte was prepared using Millipore Milli Q water (>18.3 MΩcm, TOC < 5 ppb), KOH pellets, conc. H_2SO_4, and conc. $HClO_4$ (*Suprapure; Merck, Germany*). The specific activity of the ORR is calculated from the positive going RDE polarization curves recorded at a scan rate of 50 mV s^{-1}. In order to exclusively analyze the ORR current, the RDE polarization curves were corrected by subtracting background surface oxidation and capacitive processes. This involves subtracting the CV in Ar saturated solution (obtained using the same experimental parameters, i.e., scan speed, rotation rate, potential window) from the ORR polarization curves. Furthermore, the so-called IR-drop was compensated for in the refined methodology. For this, the solution resistance between the working electrode and the Luggin capillary was determined using an AC signal (5 kHz, 5 mV) and thereafter compensated for, using the analog potentiostat's positive feedback scheme. The resulting effective solution resistance was less than 2 Ω for each experiment. The mass activity was calculated based on the specific activity and the ECSA, averaged from at least eight values with two different suspensions, each determined via CO stripping experiments using a multiarray electrode.[20] The CO stripping curves were recorded in CO-free Ar purged solution, after adsorbing CO at a potential of 0.05 V until the saturation coverage was reached. Because CO-stripping experiments in KOH solution lead to larger experimental errors, the surface area of the electrodes used in the experiments in KOH solution was determined in $HClO_4$ electrolyte, after transferring the electrode to a new cell. In all experiments a positive potential limit of 1.1 V_{RHE} was never exceeded.

Simulations. In order to compare the experimental data of the HSA carbon supported catalysts with data obtained from Pt single crystals, simulations of Pt NP activity were performed. In these simulations it is assumed that the Pt NPs are of ideal cuboctahedral shape according to ref 23 and that 30% of each particle is covered by the carbon support, i.e., is assumed inactive. The SA of the NPs is calculated by multiplying their surface averaged distribution of sites with the SA of the respective single crystal electrode facets in perchloric and sulfuric acid solution. The MA was then calculated by multiplying the calculated SA with the calculated ECSA. The single crystal activity values for the ORR were taken from the work of D. Strmcnik[24] and are listed in the Supporting Information in Table S1. The data demonstrate that, in contrast to earlier assumptions, not only the (100) crystal face is active. To our knowledge, no activity values—but only activity trends—exist for alkaline solution on single crystals. This might be related to experimental difficulties when working in alkaline solutions.[21,25] Due to this lack of reference data, we could only simulate activity trends from measurements in acid electrolyte, which nevertheless are sufficient for the discussion. Further details on the simulations can be found in the Supporting Information.

RESULTS AND DISCUSSION

We examined the influence of the electrolyte on the particle size effect of Pt for the ORR using three different electrolytes: two acid electrolytes with varying anionic adsorption strength, 0.1 mol dm^{-3} $HClO_4$ and 0.05 mol dm^{-3} H_2SO_4, as well as an alkaline electrolyte, namely 0.1 mol dm^{-3} KOH. The obtained results are summarized in Figure 1 and Table 1. Several important aspects of the particle size effect become obvious.

For all Pt catalysts the absolute value of the reaction rate, expressed as either SA or MA, clearly depends on the supporting electrolyte. The absolute reaction rates decrease in the order $HClO_4$ > KOH > H_2SO_4 in line with an increasing anionic adsorption strength in the case of the acid solutions, whereas the lower activity of KOH compared to $HClO_4$ might be due to the noncovalent interactions between hydrated K^+ and adsorbed

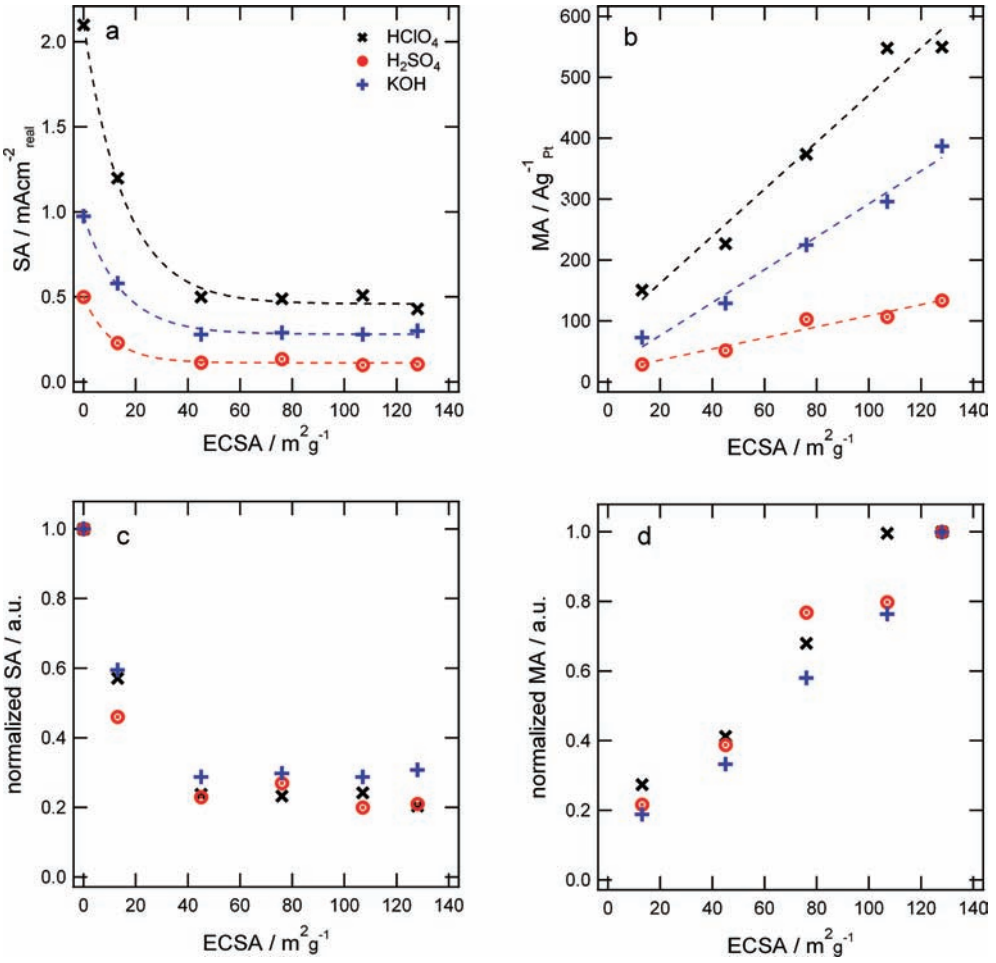

Figure 1. Specific and mass activities vs the ECSA in the different electrolytes measured at room temperature at 0.9 V vs RHE. Activities analyzed from the IR compensated positive-going sweeps at 50 mV s^{-1}, after subtraction of the capacitive background. The lines only serve as a guide to the eye. (a) Specific activities vs the ECSA. (b) Mass activities vs the ECSA. (c) Specific activities normalized to the Pt-poly activity vs the ECSA. (d) Mass activity normalized to the 1 nm catalyst vs the ECSA.

Table 1. Summary of the Properties of the Investigated Catalysts[a]

	PS, nm	Pt_L, %	ECSA, $m^2\ g^{-1}{}_{Pt}$	SA $HClO_4$, mA $cm^{-2}{}_{Pt}$	SA H_2SO_4, mA $cm^{-2}{}_{Pt}$	SA KOH, mA $cm^{-2}{}_{Pt}$	MA $HClO_4$, A $mg^{-1}{}_{Pt}$	MA H_2SO_4, A $mg^{-1}{}_{Pt}$	MA KOH, A $mg^{-1}{}_{Pt}$
HS_1	1−1.5	19.4	128	0.43	0.105	0.30	0.55	0.134	0.387
HS_2	2	20.1	108	0.51	0.1	0.28	0.548	0.107	0.296
HS_3	2−3	46	76	0.49	0.135	0.29	0.374	0.103	0.225
HS_5	4−5	50.6	46	0.5	0.115	0.28	0.227	0.052	0.129
Pt_{black}	30	96	13	1.2	0.23	0.58	0.151	0.029	0.073
Pt_{poly}	–	–	–	2.1	0.5	0.98	–	–	–

[a] PS: mean diameter of the particles; Pt_L: Platinum loading of catalyst in percent by weight; ECSA: electrochemical surface area; SA_{HClO4}: specific activity in 0.1 mol dm^{-3} $HClO_4$; SA_{H2SO4}: specific activity in 0.05 mol dm^{-3} H_2SO_4; SA_{KOH}: specific activity in 0.1 mol dm^{-3} KOH; MA_{xx}: mass activities.

OH.[26] As a consequence, it is proposed that the concept of spectator species applies not only to single crystals but also to all types of Pt based electrocatalysts. Interestingly, the observed trends in activity, i.e. the activity vs ECSA, are independent of the supporting electrolyte (and thus the anionic adsorption strength). This is highlighted in Figure 1c,d where the SAs and MAs of the catalysts in the different electrolytes have been normalized to the respective most active catalyst, i.e. polycrystalline Pt in the case of the SA[15] and HS_1 in the case of the MA.

Although there is a considerable decline in SA with decreasing particle size, the difference in SA between the four HSA carbon supported catalysts (1−5 nm) is comparatively small and lies within the experimental error of the measurements, an observation which is valid for all three different electrolytes. It is

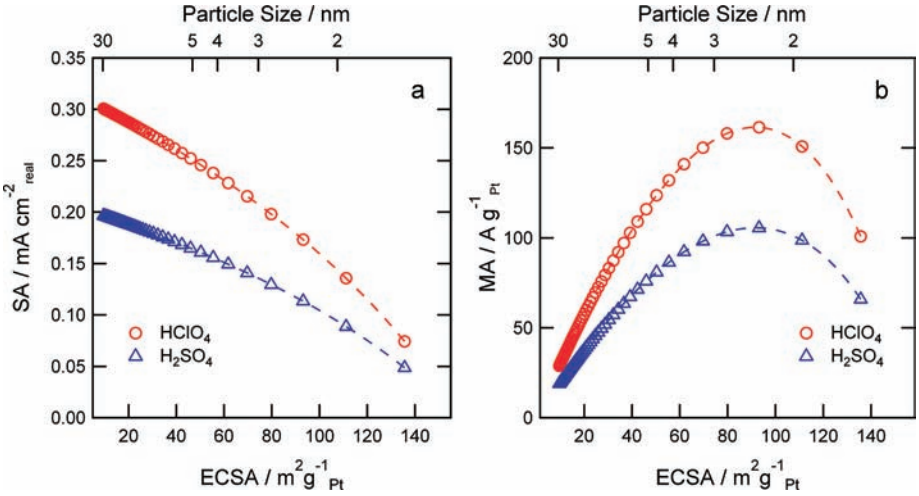

Figure 2. Simulation of expected SA (a) and MA (b) at 0.9 V_{RHE} as a function of the ECSA for perchloric and sulfuric acid solutions. It is assumed that only (100) sites are active and that 30% of the particle is covered by the support. For graphs of SA and MA vs the particle size, see Supporting Information.

noteworthy that this discrepancy between our new and previous results reported in perchloric acid solution[16]—where larger differences in the SA between the four HSA carbon supported catalysts were reported—is a direct consequence of a key improvement to the experimental protocol employed in this new study: the subtraction of the capacitive current contributions of the HSA carbon support from the overall electrode current. This refinement concerning data treatment is of particular importance to the comparison of HSA carbon supported Pt catalysts that are either of different carbon % weights or utilize various different HSA carbon supports. Explicitly, in cases where the capacitive contributions of the HSA carbon support are significant, such as at high carbon % weights and/or large HSA carbon BET areas, the cathodic ORR current observed in the positive polarization sweep is inherently shifted anodically, thereby decreasing the apparent activity of the supported NPs. It is noteworthy that without IR-drop compensation and correction for capacitive current contributions the previous activity values[16] are reobtained; however the apparent trends in the experimental data are then in danger of being misinterpreted.

In contrast to previous work,[15,16] the overall particle size effect is better characterized by a rapid decrease in the SA of the ORR going from polycrystalline Pt, to unsupported Pt black particles, and HSA carbon supported Pt NPs, i.e. $SA_{Pt\text{-}poly} \gg SA_{Pt30\ nm} \gg SA_{HSAC}$, rather than the less significant difference between the individual HSA catalysts (particle size ranging from 1 to 5 nm). Furthermore, the MA of the catalysts does not exhibit a maximum at a specific particle size/dispersion but instead continues to increase with the ECSA (see Figure 1b). It is moreover worth mentioning that in order to scrutinize if the measured increase in the SA of the larger unsupported 30 nm particles is due to a possible support effect, the unsupported Pt NPs were additionally characterized by mixing the NPs with the HSA carbon support used in the synthesis of the supported catalysts. No change in the SA could be observed.

The observed trends in SA and MA are quite intriguing for two reasons: (i) the trends are independent of the supporting electrolyte despite its strong influence on the activity of single crystal electrodes, and (ii) the difference in SA between the individual HSA carbon supported catalysts (1 to 5 nm) is rather insignificant despite the fact that the particle size effects are typically expected to occur in the low nanometer region (ca. < 5 nm) where materials start to lose their continuous bulk properties. For particle sizes below 5 nm drastic changes in the surface structure appear, a fact which was actually utilized in one of the earliest and most common explanations for the decreasing activity with particle size. According to this approach,[11] the ORR activity for different particle sizes can be modeled by combining the SA of single crystals with the surface area and mass averaged distribution of the surface crystal planes of an ideal cuboctahedron cluster. In the following section we will scrutinize this approach by comparing the experimental results with the activity trends obtained by such simulations.

In a first step, we modeled the SA and MA in the acidic supporting electrolytes given in Figure 2a and b, by assuming that only the Pt(100) planes are active for the ORR, as in Kinoshita's model.[11]

The model predicts that in both acidic electrolytes the SA declines linearly with increasing ECSA and decreasing particle size, anticipating a maximum MA for catalysts with an ECSA of ~90 $m^2\ g^{-1}$, i.e. a particle size of ca. 2.5 nm. While a discontinuous increase in MA with ECSA was reported in some experimental studies,[9,10,15] the predicted linear relationship between the SA and ECSA (see SF2 in Supporting Information for a plot vs particle size instead of ECSA) could not be observed in any experimental study so far; instead only relatively small differences in SA were observed between catalysts with particle sizes ≤5 nm.[14−17] As already highlighted, our refined measurement methodology strongly suggests that the difference in the SA of small Pt NPs reported previously can instead be attributed to differences in the capacitive current contributions of the HSA carbon support toward the overall electrode current rather than an intrinsic difference in the SA of different particle sizes. Thus, the resulting MA does not exhibit a discontinuous but a more or less linear increase with ECSA. This interpretation is consistent with a previous observation discussed by Gasteiger et al.[15] whereby a maximum in the MA at around 90 $m^2\ g^{-1}$ (in accordance to Kinoshita's model[11]) was only observed in polarization curves recorded at high scan rates, where the capacitive current contributions are inherently more significant.

dx.doi.org/10.1021/ja207016u |J. Am. Chem. Soc. 2011, 133, 17428–17433

If, in addition to (100) sites, the (111) sites are also considered in the simulation, the absolute values of SA and MA of the ORR change; however, the shape of the activities vs ECSA curve is not affected (see SF3 in Supporting Information). This is because, in a cuboctahedron model, the trends in the surface area- and mass-averaged distribution for square (100) and triangle (111) sites with particle size are the same (SF1 in Supporting Information). Furthermore, by including arbitrary contributions from the step and corner atoms to the overall ORR activity in the model by, for instance, assuming that the ORR rate on these atoms is equal to that of the (110) facet of Pt, a trend that is in even stronger disagreement with the experiments is revealed; i.e. the SA increases with increasing ECSA (see Figure SF4 in the Supporting Information). In fact, no agreement between the trend in the simulation and the experimental data can be found in order to account for the significant increase in the SA of the larger unsupported 30 nm particles by assuming different arbitrary contributions from step and corner atoms (between low and high contribution to ORR; see SF5 in the Supporting Information).

It can therefore be concluded that the common approach of correlating single crystal data with experiments on supported catalysts is not consistent. Assuming a 1:1 correlation between crystal facets of NPs in a geometric model of ideal particles and the overall ORR activity of the catalyst will always lead to the most drastic changes for rather small particles and not surfaces with low ECSA. This is in clear contradiction to the measured trends in catalyst activity observed in the majority of investigations. Therefore, despite that the catalyst surface structure undoubtedly influences the kinetics of the ORR, the relationship between single crystal systems and NP catalysts remains unresolved. As a consequence alternative/refined models need to be found that are able to explain the full spectra of experimental results of carbon supported Pt NPs. Scrutinizing such models, possible directions could be (i) that the majority of the Pt NPs in the industrial catalysts are not the active centers crucial for the ORR but rather smaller Pt clusters, as reported for the case of CO oxidation on Au NP;[27] (ii) that oxygen mass transfer particularly in micropores influences the apparent activities; (iii) that the support influences the activity, e.g. by imposing structural constraints on the Pt NPs; or (iv) that the effective reaction pathway of the ORR changes with the particle size. Although definitively necessary for demonstrating and understanding particle size effects in real applications, measurements on commercial HSA carbon supported catalysts alone might not be sufficient to clarify all remaining open questions. The disadvantages of these catalysts lay at hand, i.e., the size distribution of the particles, the microporosity of the support, and the interaction of support and catalyst particles. Consequently we started studies on more defined catalyst systems as well. However, in our ongoing work[28,29] on unsupported Pt nanoclusters created by a laser ablation source,[30] size selected and deposited onto a planar carbon substrate, we so far found no indication that mass transfer constraints or small Pt nanoclusters are responsible for the behavior of industrial catalysts. Instead specific ORR activities on these nanocluster samples are almost identical, i.e. 0.6 mA cm^{-2},[28] to the ones of the commercial supported catalysts. Another interesting approach for model studies is the fabrication of well-defined, shaped Pt nanocrystals by using electron beam lithography,[31] which can be seen as a link between the extended single crystals and undefined supported nanoparticles. Systems like these, eventually also applied onto an HSA support, will help to elucidate the unexpected particle size trend for the ORR.

CONCLUSION

The effect of particle size on the ORR activity of Pt was carefully examined in three different electrolytes. The activity trend for the ORR with changing particle size is independent of the electrolyte and rapidly decreases going from polycrystalline Pt, to unsupported Pt black particles, and HSA carbon supported Pt NPs, i.e. $SA_{Pt\text{-}poly} \gg SA_{Pt30\ nm} \gg SA_{HSAC}$. While the influence of spectator species does inflict significantly different absolute reaction rates in the different electrolytes, the observed trend is independent of the anionic adsorption strength of the acid electrolyte. In contrast to previous work, it is found that the difference in SA between the individual HSA carbon supported catalysts is very small and within the error of measurements; instead, the differences in activities reported previously can be attributed to different capacitive current contributions toward the overall electrode current. In all of the investigated electrolyte solutions the MA increases with increasing catalyst dispersion. The prevailing particle size effect models, which are based on a straightforward correlation between single crystal results and the properties of supported nanoparticle electrocatalysts, only predict a strong particle size effect for small particles <5 nm and almost no effect for the large NPs > 10 nm. This is clearly not in agreement with the experimental findings, and the models can therefore be concluded to be insufficient in predicting the behavior of nanoparticle catalysts. Further investigations will be necessary in order to fully understand the particle size effect for the ORR, in particular to rationalize the large difference in the activity observed between polycrystalline Pt and high surface area catalysts, and to exclude any influence of the catalyst support. For such studies, improved simulations along with nanoparticle catalysts that are more defined than the industrial catalysts used here will be necessary.

ASSOCIATED CONTENT

Supporting Information. Detailed information about the simulated SA and MA and additional results considering different active atom sites, TEM micrographs of the HSA carbon supported catalysts and the Pt black catalyst. This material is available free of charge via the Internet at http://pubs.acs.org.

AUTHOR INFORMATION

Corresponding Author
m.arenz@chem.ku.dk

ACKNOWLEDGMENT

This work was supported by the German DFG through the Emmy-Noether Project ARE852/1-1. J.C.M. acknowledges financial support by the Kekulé Fellowship from the Fonds der Chemischen Industrie (FCI). The authors furthermore acknowledge supporting measurements from Andres Novo Nunez.

REFERENCES

(1) Ertl, G. *Angew. Chem., Int. Ed.* **2008**, *47*, 3524.
(2) Somorjai, G. A. *Surf. Sci.* **1994**, *299*, 849.
(3) Markovic, N. M.; Ross, P. N. *Surf. Sci. Rep.* **2002**, *45*, 121.
(4) Markovic, N. M.; Gasteiger, H. A.; Ross, P. N. *J. Phys. Chem.* **1995**, *99*, 3411.

(5) Stamenkovic, V. R.; Mun, B. S.; Arenz, M.; Mayrhofer, K. J. J.; Lucas, C. A.; Wang, G. F.; Ross, P. N.; Markovic, N. M. *Nat. Mater.* **2007**, *6*, 241.
(6) Markovic, N. M.; Adzic, R. R.; Cahan, B. D.; Yeager, E. B. *J. Electroanal. Chem.* **1994**, *377*, 249.
(7) Boudart, M. *Adv. Catal.* **1969**, *20*, 153.
(8) Greeley, J.; Rossmeisl, J.; Hellman, A.; Norskov, J. K. *Zeitschrift Fur Physikalische Chemie-International Journal of Research in Physical Chemistry & Chemical Physics* **2007**, *221*, 1209.
(9) Sattler, M. L.; Ross, P. N. *Ultramicroscopy* **1986**, *20*, 21.
(10) Peuckert, M.; Yoneda, T.; Betta, R. A. D.; Boudart, M. *J. Electrochem. Soc.* **1986**, *133*, 944.
(11) Kinoshita, K. *J. Electrochem. Soc.* **1990**, *137*, 845.
(12) Romanows., W *Surf. Sci.* **1969**, *18*, 373.
(13) Vanharde., R; Hartog, F. *Surf. Sci.* **1969**, *15*, 189.
(14) Takasu, Y.; Ohashi, N.; Zhang, X. G.; Murakami, Y.; Minagawa, H.; Sato, S.; Yahikozawa, K. *Electrochim. Acta* **1996**, *41*, 2595.
(15) Gasteiger, H. A.; Kocha, S. S.; Sompalli, B.; Wagner, F. T. *Appl. Catal., B* **2005**, *56*, 9.
(16) Mayrhofer, K. J. J.; Blizanac, B. B.; Arenz, M.; Stamenkovic, V. R.; Ross, P. N.; Markovic, N. M. *J. Phys. Chem. B* **2005**, *109*, 14433.
(17) Mayrhofer, K. J. J.; Strmcnik, D.; Blizanac, B. B.; Stamenkovic, V.; Arenz, M.; Markovic, N. M. *Electrochim. Acta* **2008**, *53*, 3181.
(18) Ye, H.; Crooks, J. A.; Crooks, R. M. *Langmuir* **2007**, *23*, 11901.
(19) Schmidt, T. J.; Gasteiger, H. A.; Stab, G. D.; Urban, P. M.; Kolb, D. M.; Behm, R. J. *J. Electrochem. Soc.* **1998**, *145*, 2354.
(20) Wiberg, G. K. H. PhD thesis, Technische Universität München, 2010.
(21) Wiberg, G. K. H.; Mayrhofer, K. J. J.; Arenz, M. *Fuel Cells* **2010**, *10*, 575.
(22) Arenz, M.; Mayrhofer, K. J. J.; Stamenkovic, V.; Blizanac, B. B.; Tomoyuki, T.; Ross, P. N.; Markovic, N. M. *J. Am. Chem. Soc.* **2005**, *127*, 6819.
(23) Montejano-Carrizales, J. M.; Aguilera-Granja, F.; Moran-Lopez, J. L. *Nanostructured Materials* **1997**, *8*, 269.
(24) Strmčnik, D. PhD thesis, Univerza v Ljubljani, 2007.
(25) Mayrhofer, K. J. J.; Wiberg, G. K. H.; Arenz, M. *J. Electrochem. Soc.* **2008**, *155*, P1.
(26) Strmcnik, D.; Kodama, K.; van der Vliet, D.; Greeley, J.; Stamenkovic, V. R.; Markovic, N. M. *Nat. Chem.* **2009**, *1*, 466.
(27) Herzing, A. A.; Kiely, C. J.; Carley, A. F.; Landon, P.; Hutchings, G. J. *Science* **2008**, *321*, 1331.
(28) Kunz, S.; Hartl, K.; Nesselberger, M.; Schweinberger, F. F.; Kwon, G.; Hanzlik, M.; Mayrhofer, K. J. J.; Heiz, U.; Arenz, M. *Phys. Chem. Chem. Phys.* **2010**, *12*, 10288.
(29) Hartl, K.; Nesselberger, M.; Mayrhofer, K. J. J.; Kunz, S.; Schweinberger, F. F.; Kwon, G.; Hanzlik, M.; Heiz, U.; Arenz, M. *Electrochim. Acta* **2010**, *56*, 810.
(30) Heiz, U.; Vanolli, F.; Trento, L.; Schneider, W. D. *Rev. Sci. Instrum.* **1997**, *68*, 1986.
(31) Komanicky, V.; Iddir, H.; Chang, K. C.; Menzel, A.; Karapetrov, G.; Hennessy, D.; Zapol, P.; You, H. *J. Am. Chem. Soc.* **2009**, *131*, 5732.